Chamber Evaluation of Process Diagnostics and Photochemical Indicators

Gail S. Tonnesen
University of California, Riverside
College of Engineering Center for Environmental Research and Technology
Riverside, CA 92521

Introduction

Historically photochemical mechanisms and air quality models have been evaluated primarily in terms of there ability to simulate observed O_3 data. There is an increasing awareness that mechanism and models must also be evaluated in terms of their ability to simulate the fundamental chemical processes that control O_3 formation and the sensitivity of O_3 to emissions reductions (Arnold et al., 1998). Such evaluative methods include process diagnostics which are useful for characterizing O_3 photochemistry (Jeffries and Tonnesen, 1994), and photochemical indicators which can be used to characterize O_3 sensitivity to VOC and NO_x (Milford et al., 1994; Sillman, 1995; Chang et al., 1997; Blanchard et al., 1999; Tonnesen and Dennis, 1999). Both of these approaches are currently being used in diagnostic model evaluations (e.g., Sillman et al., 1997a,b, 1998; Imre et al, 1999). There are considerable uncertainties, however, in the usefulness of these methods due to uncertainties in each of the many sink and source terms that can contribute to production or loss of trace species. For example, there are uncertainties of 20% or more in important gas phase reactions (Donahue et al, 1997; Gao et al., 1995, 1996), large uncertainties in heterogeneous chemistry (Dentener and Crutzen, 1994) and in emissions inventories, deposition rates and transport. Because of these uncertainties, it can be difficult to use ambient data to validate model simulations of chemical processes. Furthermore, the particular values of photochemical indicators that distinguish NO_x sensitive or VOC sensitive conditions have only been derived from model simulations. To date there has been no empirical validation of the usefulness of these indicators. Here we propose that before process diagnostics and photochemical indicators can be used with confidence in model evaluations, their behavior must be characterized under the relatively well controlled conditions of chamber experiments. Each of these approaches is discussed below, and the measurements necessary to evaluate them in chamber experiments are listed.

Definitions

Reactive odd nitrogen (NO_x) is traditionally defined as the sum of NO + NO_2. There are, however, several other reactive forms of odd nitrogen which participate in O_3 and PM photochemistry where these include nitrous acid (HONO), the nitrate radical (NO_3), dintrogen pentoxide (N_2O_5), peroxynitric acid (HNO_4). These species typically have low concentrations for daytime photochemistry, but for completeness the total sum of reactive odd nitrogen can be defined as NOX (e.g., Dentener and Crutzen, 1994):

$$NOX = NO + NO_2 + NO_3 + 2\ N_2O_5 + HONO + HNO_4$$

The relatively inert forms of odd nitrogen (NO_z) can then be defined as the sum of nitric acid (HNO_3), organic nitrates (RNO_3), particulate nitrate (NO_3-), and peroxyacetyl nitrates (PAN):

$$NO_z = HNO_3 + RNO_3 + NO_3^- + PAN$$

And then total odd nitrogen (NO_y) can be defined as

$$NO_y = NOX + NO_z$$

For convenience HC will be defined as the sum of all species that can react with OH to produce O_3. Thus, HC includes VOC, methane, carbon monoxide and biogenic carbon. The family of odd oxygen (O_x) is the sum of all species that can act as reservoirs for atomic oxygen

$$O_x = O_3 + O^1D + O^3P + NO_2 + 2\ NO_3 + 3\ N_2O_5 + HNO_4 + HNO_3 + RNO_3 + NO_3^- + PAN$$

Production of O_x in the troposphere occurs almost exclusively by the reaction of NO with peroxy radicals (HO2 and RO2):

(R1) $NO + HO_2 \rightarrow NO_2 + OH$

(R2) $NO + RO_2 \rightarrow NO_2 + RO$

so gross production of O_z can be defined as the rate of reaction of NO with HO_2 and RO_2

$$P_G(O_z) = k_1\ NO\ HO_2 + k_1\ NO\ RO_2$$

There is also some photochemical destruction of O_z (L_{Ox}), so net production of O_z can be defined as:

$$P(O_z) = P_G(O_z) - L_{Ox}$$

This definition is identical to Rsmog as defined by Johnson (1984), and this definition is convenient because $P(O_x)$ can be evaluated through ambient measurements as the production of O_3 plus the amount of NO oxidized to other forms of NO_y. It is also convenient to define HC as the sum of all species that can react with OH to produce O_z:

$$HC = VOC + biogenic\ VOC + CO + CH_4$$

Process Diagnostics

Figure 1 illustrates most of the important components of the chemical processes that control the photochemical formation of O_3. The first step in O_3 production is the initiation of new radicals. In the models, the primarily source of radical initiation is photolysis of HCHO and O_3, with a lesser contribution by photolysis or decomposition of other radical precursors. There is uncertainty, however, whether the these "minor" radical sources are accurately represented in air quality models. For example, HONO may be a significant source of radical initiation particularly in early mornings (Kleffman et al., 1998).

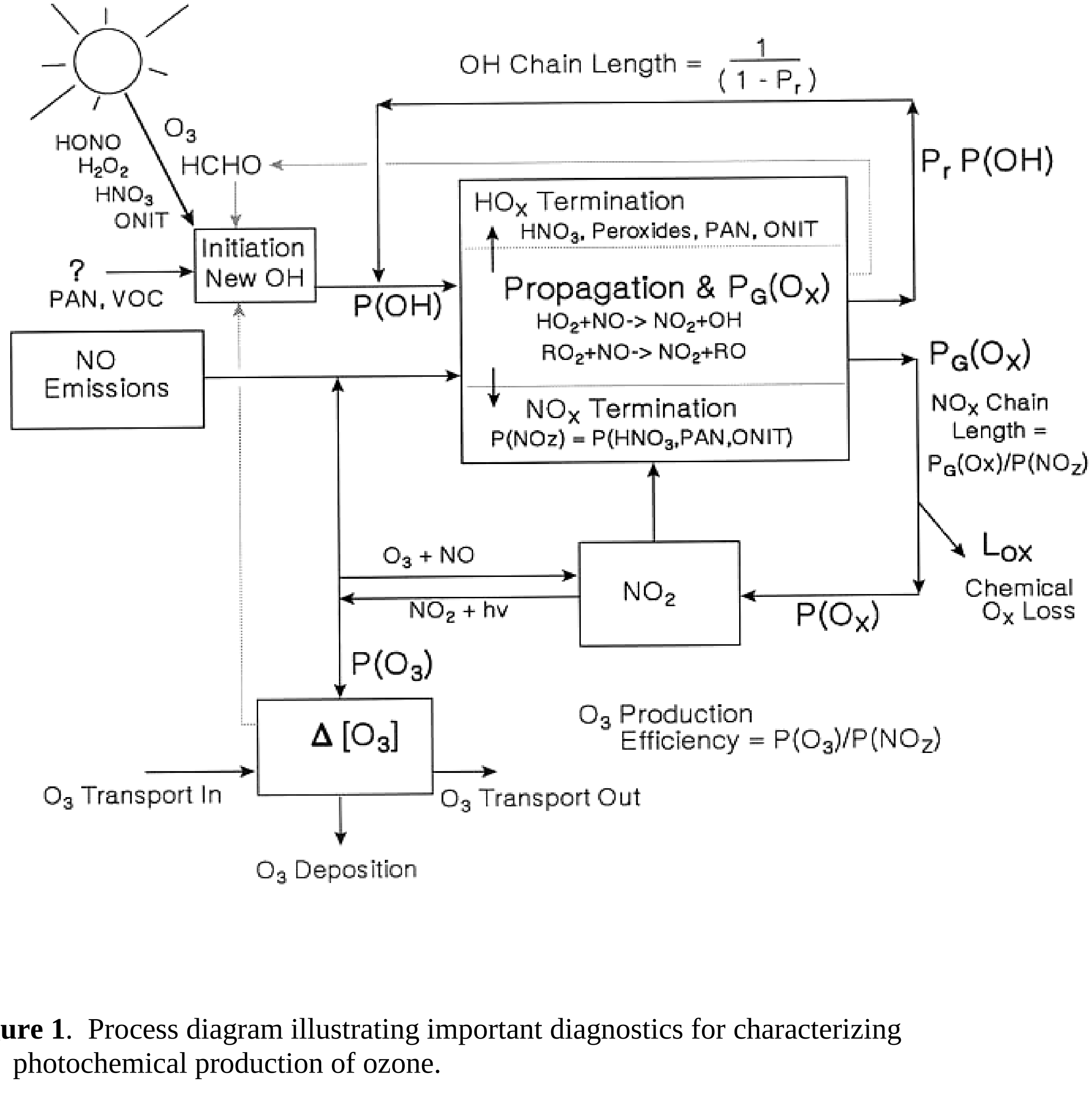

Figure 1. Process diagram illustrating important diagnostics for characterizing photochemical production of ozone.

Radicals may be produced directly in the form of OH, or as HO_2 and RO_2 followed by conversion to OH via R1 or R2. OH radicals can then attack HC to produce peroxy radical which can react with NO to produce O_x in the form of NO_2, and also recreate the OH radical.

The OH propagation efficiency, Pr_{OH} is the fraction of OH recreated for each OH that reacts. The propagation efficiency is always less than one because radicals are also destroyed in termination reactions that produce peroxides or that convert NO*X* to NOz. The OH chain length is the average number of times a new radical cycles through the chain reaction until being removed in a termination reaction, and the chain length can be calculated as:

$$\begin{aligned}\text{OH chain length} &= 1 + Pr_{OH} + Pr_{OH}^{2} + Pr_{OH}^{3} + \ \dots \\ &= 1/(1-Pr_{OH})\end{aligned}$$

The OH chain length acts as a multiplier so that total OH production *P*(OH) is the product of the OH chain length multiplied by OH initiation.

The result of this sequence of reactions is some gross production of odd oxygen, some of which is lost by photochemical destruction, and some net production $P(O_x)$ which is initially expressed in the form of NO_2. But because O_3, NO_2 and NO exist in a photostationary-state equilibrium, some of this NO_2 will photolyze to produce O_3 thereby recreating an NO that can go on to produce more O_x. The NO_x chain length can be defined as the average number of NO to NO_2 conversions mediated by a molecule of NOx before it is converted to inert NO_z. It is important to note that it is difficult to explain the processes that contribute to peak O_3 levels simply by evaluating production of O_3 – a more complete characterization of the photochemical dynamics is obtained by evaluating the total budget of O_x and then explaining the resulting peak O_3 level as the amount of O_x that remains after oxidation of NO emissions.

Local and Cumulative Diagnostics

It is also useful to distinguish between local diagnostics and cumulative diagnostics. Local diagnostic refers to the instantaneous chemical production rates, e.g., the rate of production of radicals or O_x, or ratios of production rates. Local diagnostics can not be evaluated by analyzing ambient concentration time-series of a product species at a given site because it is impossible to distinguish the relative contributions of chemistry and transport to changes in the concentration of the product species. Local diagnostics can be evaluated, however, by measuring the concentrations of the reactant species and then using the rate constants to calculate the instantaneous production rates. An example would be using actinic flux and ambient concentrations of O_3 and H_2O to estimate the local production rate of OH radicals from O_3 photolysis.

Cumulative diagnostics include those species concentrations that characterize cumulative production rates integrated over a period of hours or days. Examples of these would be using the concentration of O_3, NO_2 and NO_z as a measure of the cumulative net production of O_x integrated over an air parcel's trajectory.

Several field studies have also made detailed measurements of OH, HO_2 and RO_2 to attempt to characterize radical budgets, and in each case the measurements have failed to agree with the models simulations (Crosley, 1997; Stevens et al., 1997; Cantrell et al., 1997). Thus there is a great deal of uncertainty in radical budgets, and an important research need is to attempt to characterize radical budgets in a controlled setting.

Environmental chambers provide an ideal opportunity for characterizing radical budgets for a number of reasons. Chamber conditions and concentrations of precursors can be carefully controlled and varied for a range of conditions of interest; chambers use a confined volume of air so that interactions between transport and chemistry do not complicate the analysis; and sophisticated equipment can be quality controlled and operated more easily in a laboratory setting compared to field experiments. An additional advantage of studying process diagnostics in a chamber is that the confined volume of air allows for time integrals of measured local diagnostics to be compared directly to measurements of the cumulative diagnostics. Finally, new chamber experiments must be performed to evaluate process diagnostics and photochemical indicators because the existing chamber data base is at high VOC and NO_x concentrations and because the existing data base lacks many of the necessary measurements, particularly measurements of NO_2, HNO_3 and peroxides, and radicals.

Wall effects will continue to be a problem in chambers studies (Carter et al., 1982; Jeffries et al., 1990), but it may be possible to minimize such effects in a low-NO_x chamber (e.g., Bailey et al., 1996; Simonaitis et al., 1995), and hopefully wall effects can be better characterized with the more sophisticated set of measurements that are becoming available in chamber facilities in the U.S. and Europe.

Photochemical Indicators

The motivation for the development of photochemical indicators is the desire for measurements that will determine whether air quality models are faithfully simulating real-world sensitivity of O_3 to changes in precursor emissions. In terms of an ozone isopleth diagram, illustrated in Figure 2 (top), indicators are used to locate ambient conditions relative to the $[O_3]$ ridge line or the $P(O_x)$ ridgeline which are defined, respectively, as:

$$\frac{\partial[\mathrm{O_3}]}{\partial E_{\mathrm{NO}_x}} = 0 \qquad \text{and} \qquad \frac{\partial P(\mathrm{O}_x)}{\partial E_{\mathrm{NO}_x}} = 0$$

where $E_{\mathrm{NO}x}$ represents emissions of NO_x. Alternatively, indicators can be defined for conditions of equal sensitivity to VOC and NO_x:

$$\frac{\partial[\mathrm{O_3}]}{\partial E_{\mathrm{NO}_x}} = \frac{\partial[\mathrm{O_3}]}{\partial E_{\mathrm{VOC}}} \qquad \text{and} \qquad \frac{\partial P(\mathrm{O}_x)}{\partial E_{\mathrm{NO}_x}} = \frac{\partial P(\mathrm{O}_x)}{\partial E_{\mathrm{VOC}}}$$

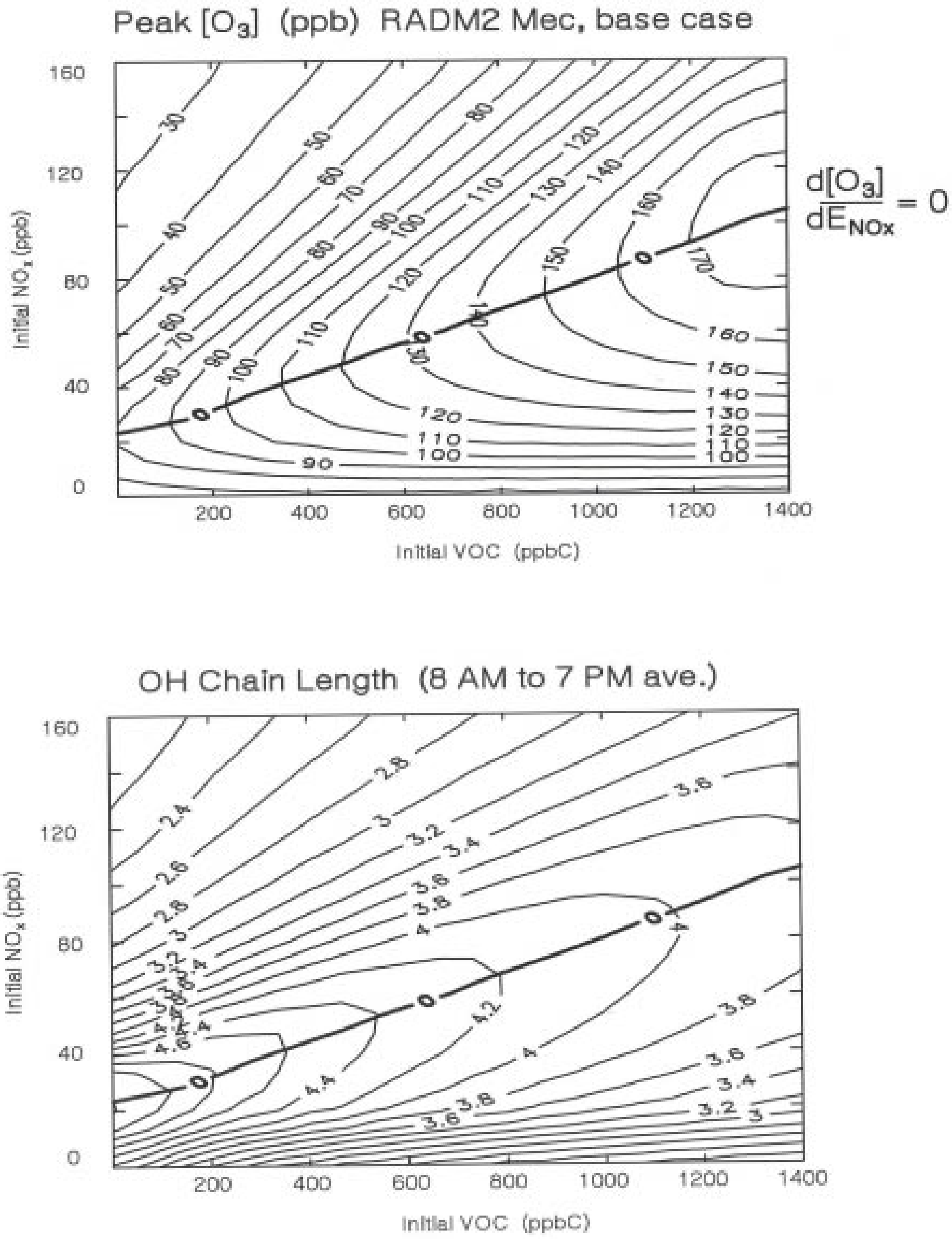

Figure 2. Response surface plots showing constant contours of O_3 (top) and the OH chain length (bottom) as a function of VOC and NOx emissions levels.

Indicators cannot replace models because indicators do not characterize the overall effectiveness of a control strategy, or whether it's even possible to attain air quality standards with a given strategy. Indicators are, however, an extremely important step in helping to decide whether the models are useful for evaluating control strategies. The theoretical basis for the usefulness of indicators has been derived by several approaches: First, the extent parameter is based on work by Johnson (1994) that characterizes the extent to which NO_x has been utilized to achieve the maximum potential O_3 formation. Secondly, Sillman (1995) and Kleinman et al. (1997) have derived indicators of $[O_3]$ sensitivity based on an analysis of the steady-state radical budgets, i.e., the observation that the rate of new radical initiation must be balanced by the rate of radical termination. And finally, Tonnesen and Dennis have derived indicators of $P(O_x)$ and $[O_3]$ sensitivity using an analysis of radical propagation efficiency (Tonnesen and Dennis, 1999a,b). The latter approach is summarized next.

The increase in O_3 concentration due to photochemistry can be assumed to be approximately proportional to the integral of $P(O_x)$, and $P(O_x)$ is approximately proportional to the rate of OH attack on HC. As discussed above, production of radicals is equal to the rate of radical initiation multiplied by the OH chain length. Because the chainlength has a $1/(1-Pr_{OH})$ dependence on propagation efficiency, the chain length increases rapidly as propagation efficiency increases and it is the dominant term that controls the rate of $P(O_x)$. As a result, the sensitivity of $P(O_x)$ to precursor emissions will be determined primarily by the sensitivity of the OH chain length, and $[O_3]$ sensitivity will be determined primarily by the sensitivity of the integral of the OH chainlength.

Figure 2 (bottom) shows the response for the OH chain length (integrated over a 12 hour model simulation) for the same set of trajectory model simulations that were used to create the $[O_3]$ response surface in Figure 2 (top). The $[O_3]$ ridgeline is also superimposed on Figure 2 (bottom) to illustrate its correlation with the area of maximum OH chain length. Figure 2 shows that the $[O_3]$ ridgeline corresponds almost exactly to a ridgeline of maximum chainlength, but there is no particular value of the chainlength that uniquely identifies the VOC or NO_x sensitive condition, for example, a chainlength of 4 could be NO_x-limited (below the ridgeline), on the ridgeline, or radical-limited (above the ridgeline). Thus, the OH chain length is not useful for distinguishing NO_x sensitive versus VOC sensitive conditions.

The individual propagation terms that control the OH chainlength, however, are useful as indicators of $[O_3]$ and $P(O_x)$ Figure 3 illustrates major radical propagation and termination pathways in the photochemical mechanism. The OH propagation efficiency can be calculated approximately as the product of the fraction of OH radicals that attack HC (f_{OH+HC}) multiplied by the fraction of subsequent HO_2 radicals that react with NO (f_{HO2+NO}) to recreate an OH radical. These two terms have an opposite dependence on NO_x. As NO_x increases, f_{HO2+NO} increases but f_{OH+HC} decreases. The result is that propagation efficiency is maximized for some intermediate level of NO_x that maximizes the product of these two terms, thereby creating the O_3 ridgeline. The values of the propagation terms can be calculated using the concentrations of the radical species, NO,

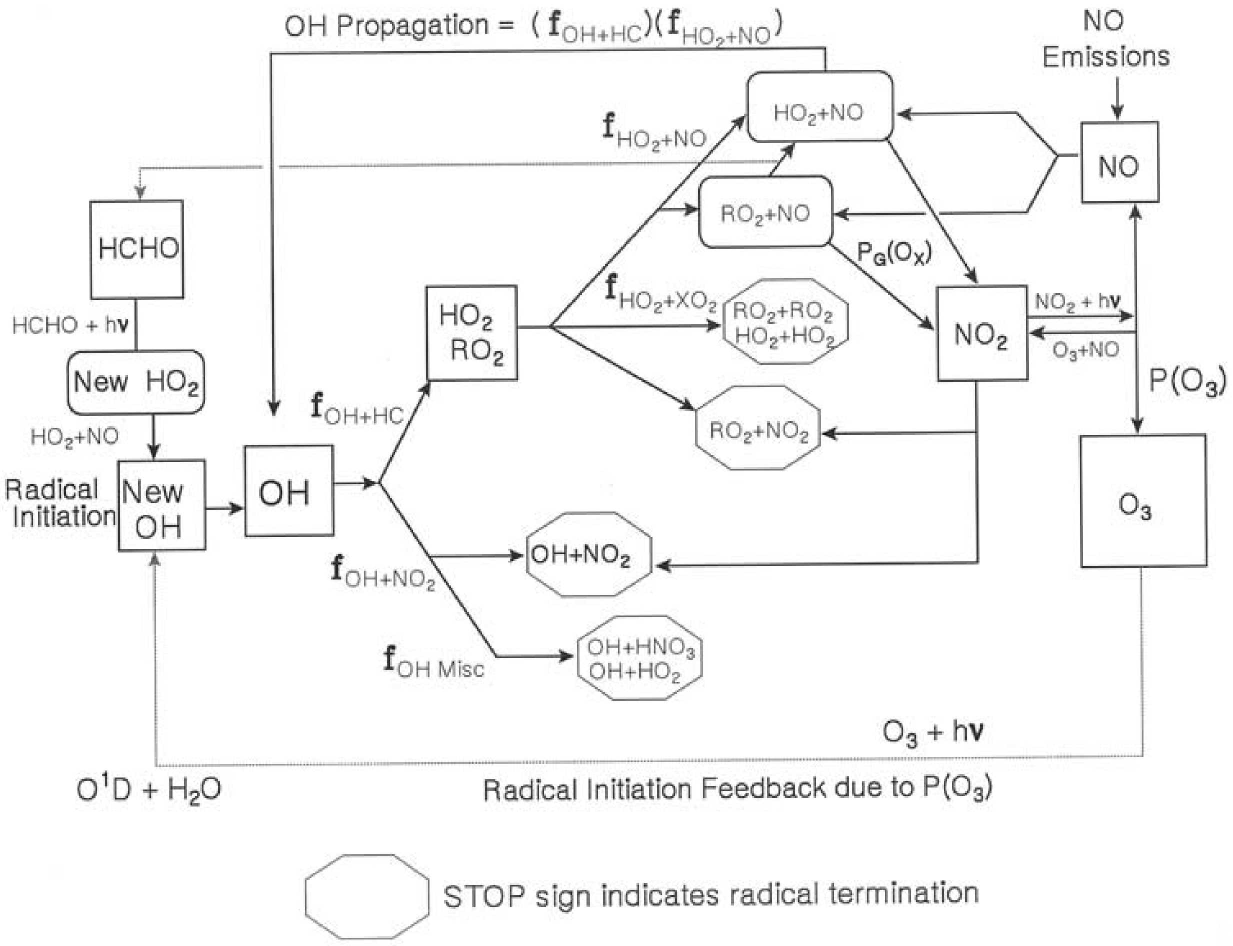

Figure 3. Radical propagation and termination pathways.

NO_2, and HC (Tonnesen and Dennis, 1999) and these propagation terms are expected to uniquely distinguish VOC sensitive and NO_x sensitive conditions.

Several approximations have been made in the derivation described above. The effects of these approximations can be numerically evaluated by using model simulations with a Gear solver to simulate the robustness of the correlation of the propagation terms with the ridgeline. Figure 4 illustrates the response surfaces for the propagation terms where the [O_3] ridgeline is again superimposed on each plot. Figure 4 (top) shows that a nearly constant $f_{HO2+NO} = 92\%$ does uniquely identify NO_x-limited and radical-limited conditions, and its value increases from about 72% at high VOC/NO_x to 100% at low VOC/NO_x conditions. Similarly, Figure 4 (bottom) shows a strong correlation of f_{OH+HC} with the ridgeline.

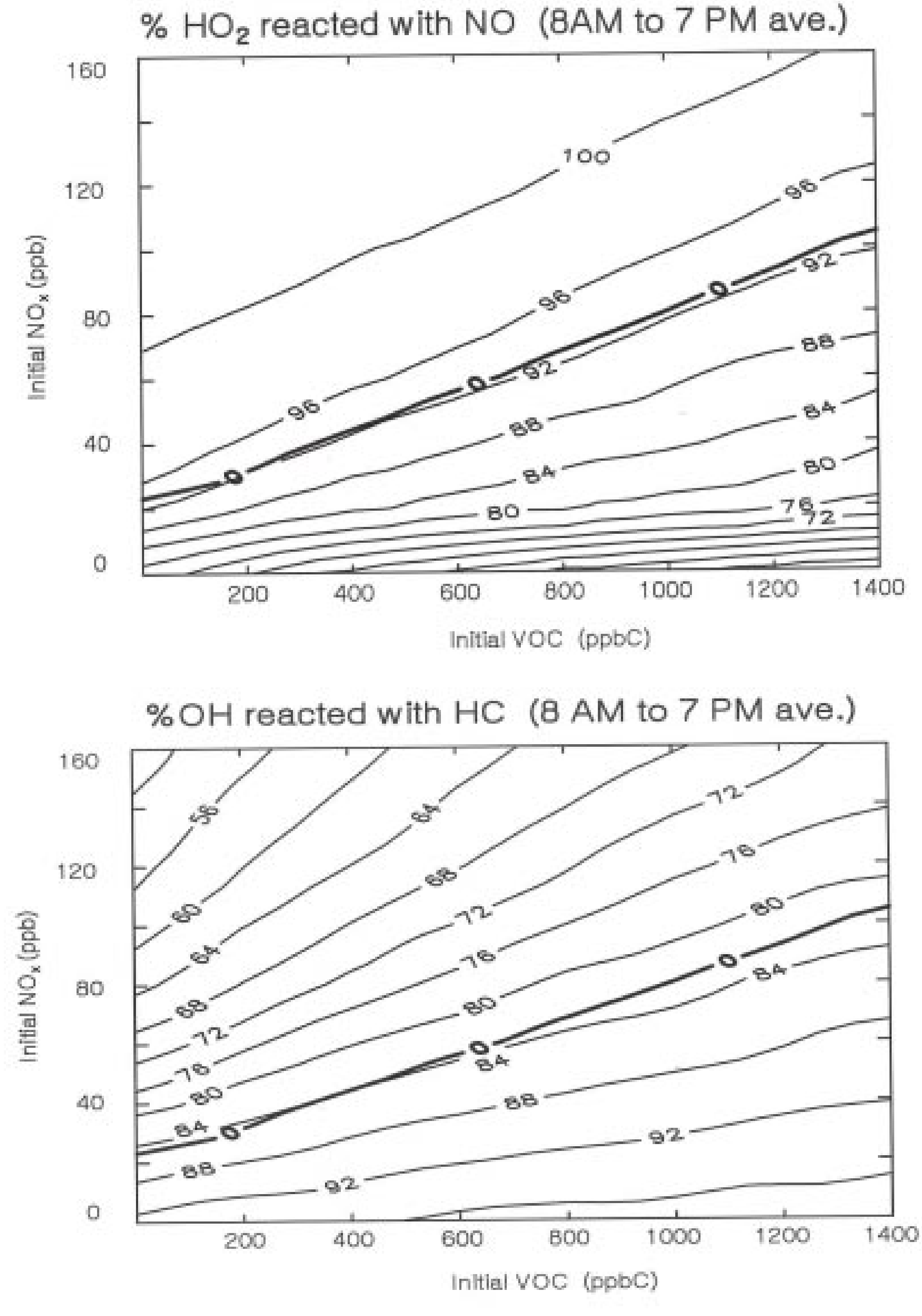

Figure 4. Response surface for propagation pathway fractions. (top) Fraction of HO_2 reacting with NO to recreate OH. (bottom) Fraction of OH attacking HC. The bold line represents the $[O_3]$ ridgeline.

A number of indicators can be derived from this analysis for $P(O_x)$ sensitivity (Tonnesen and Dennis, 1999a) and for $[O_3]$ sensitivity (Tonnesen and Dennis,1999b) including some of those previously proposed by Sillman (1995) for $[O_3]$ sensitivity. Each of these indicators were evaluated in simulations of the Regional Acid Deposition Model (Tonnesen and Dennis, 1999a,b). It was found that the indicators performed best for sunny conditions with high O_3 levels. They were less reliable, however, for conditions where clouds reduced the photorates or where deposition and heterogeneous chemistry affected the concentrations of O_3 and radical termination products.

Although uncertainty remains in the robustness of indicators, there is nonetheless a strong theoretical basis for their usefulness. It is potentially the most powerful method to date for evaluating the accuracy of model simulated sensitivity of O_3 to changes in precursors. Due to uncertainties in the chemistry and other atmospheric processes, air quality models are inadequate for characterizing indicators. Validation of the indicator concept and determination of the particular values that correlate with the ridgeline must be experimentally validated under controlled conditions where precursor emissions can be perturbed and the O_3 response measured for a wide range of conditions. Such experiments could be performed either in chamber experiment or in field studies using captured ambient air.

In a chamber study, a large number of simulations could be performed to map out the response surfaces for $[O_3]$, $P(O_x)$ and each of the indicators, as illustrated in Figure 5.

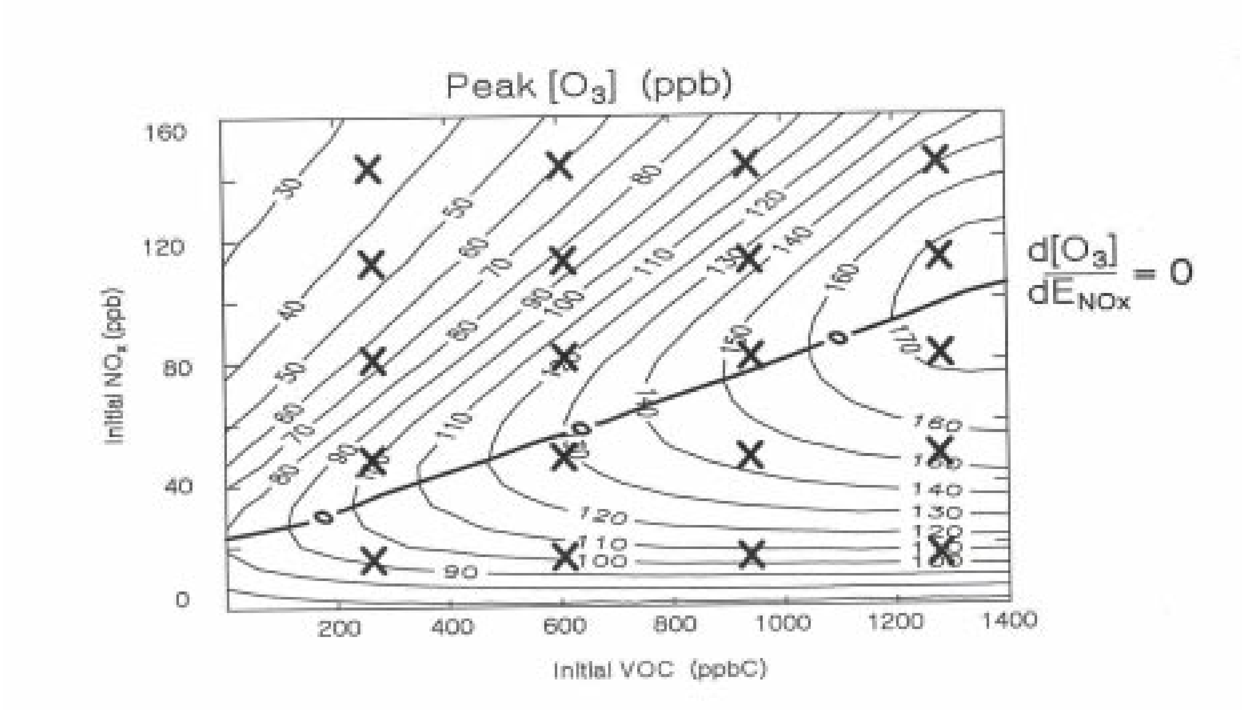

Figure 5. Illustrates the range of conditions needed in a chamber experiments to map out the response surface for O_3 and the indicators.

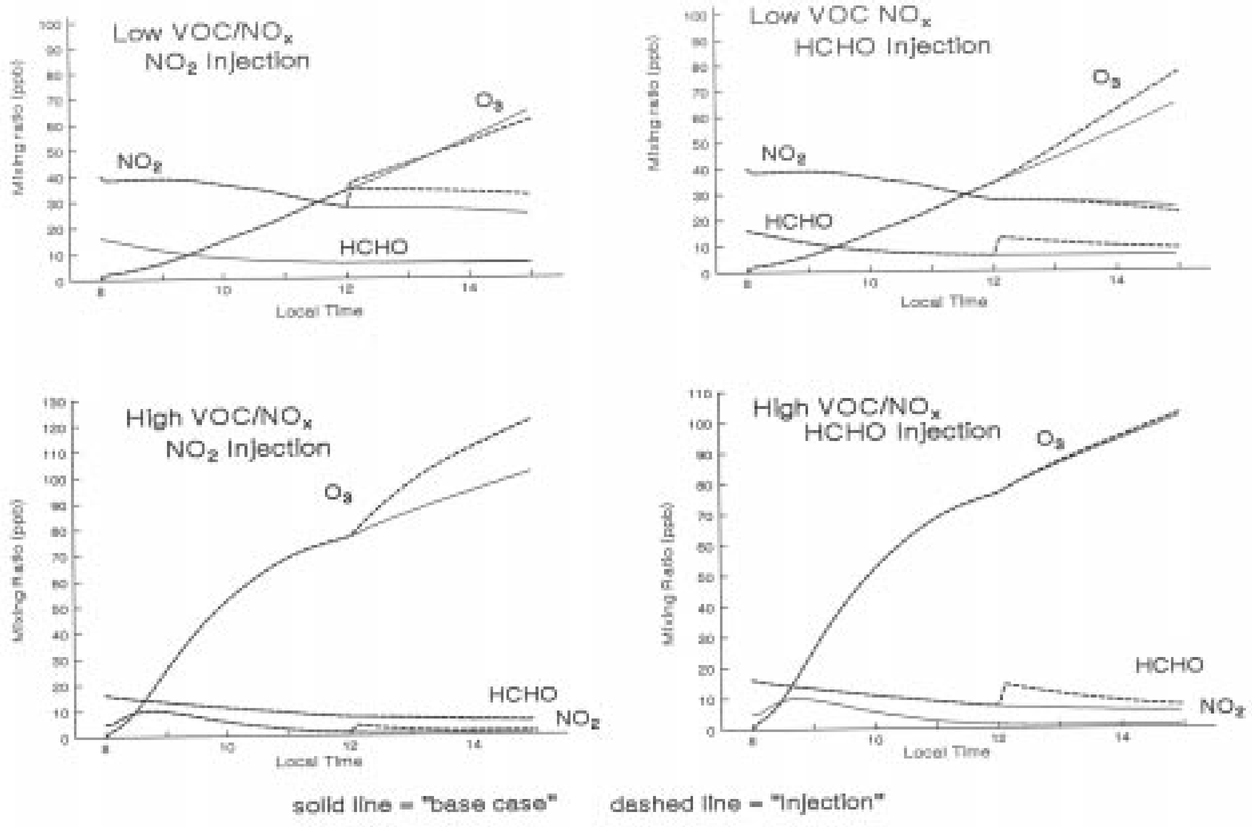

Figure 6. Model simulations of O3 response to NO2 and HCHO injections in a simulated "captive air" experiment.

Alternatively, a more limited experiment could be performed in a field study using three portable chambers to capture ambient air. One chamber would be used as a null case, and NO$_x$ or HCHO (as radical source) would be injected into the remaining two chambers (e.g., Kelly, 1985). The system response would be determined by comparing the changes in O$_3$ and P(O$_x$) in each of the bags to the null case. Figure 6 illustrates the results of a mode simulation of such an experiment. If this an experiment were "piggy-backed" on a supersite in a field study, measurements of many of the indicators could be obtained, and their correlation with the O$_3$ response could then be evaluated.

Conclusions

There is great interest and considerable potential in using process diagnostics and photochemical indicators to improve our confidence in the accuracy and usefulness of air quality model simulations. Large uncertainties remain, however, in the interpretation of the ambient data for elucidating atmospheric processes and in the robustness of these methods. Evaluation of these methods in the carefully controlled conditions of environmental chambers could provide a significant improvement in our ability to evaluate air quality models.

References

Arnold, J.R.; Dennis, R.L.; and Tonnesen, G.S. (1998) Advanced techniques for evaluating Eulerian air quality models: background and methodology. In: Preprints of the 10th Joint Conference on the Applications of Air Pollution Meteorology with the Air & Waste Management Association, January 11-16, 1998, Phoenix, Arizona. American Meteorological Society, Boston, Massachusetts, paper no. 1.1, pp. 1-5.

Bailey, E.M.; Copeland, C.H.; and Simonaitis, R. (1996) Smog chamber studies at low VOC and NO_x concentrations. Report on Interagency Agreement DW64936024 to EPA/NREL, Research Triangle Park, NC.

Blanchard, C.L.; Lurmann, F.W.; Roth, P.M.; Jeffries, H.E.; and M. Korc (1999). The use of ambient data to corroborate analyses of ozone control strategies. *Atmospheric Environment* (in press).

Cantrell, C.A.; Shetter, R.E.; Calvert, J.G.; Eisele, F.L.; Williams, E.; Baumann, K.; Brune, W.H.; Stevens, P.S.; and Mather, J.H. (1997) Peroxy radicals from photostationary state deviations and steady state calculations during the Tropospheric OH Photochemistry Experiment at Idaho Hill, Colorado. *J. Geophys. Res. 102***:**6369-6378.

Carter, W.P.L.; Atkinson, R.; Winer, A.M.; and Pitts, J.N., Jr. (1982) Experimental investigation of chamber-dependent radical sources. *Int. J. Chem. Kinet. 14***:**1071.

Chang, T. Y., D. P. Chock, B. I. Nance, and S. L. Winkler (1997) A photochemical extent parameter to aid ozone air quality management, *Atmos. Environ., 31*, 2787-2794.

Crosley, D. R.(1997) The 1993 tropospheric OH photochemistry experiment: A summary and perspective, *J. Geophys. Res., 102*, 6495-6510.

Dentener, F. J., and P. J. Crutzen (1993) Reaction of N_2O_5 on tropospheric aerosols: Impact on global distributions of NO_x, O_3, and OH, *J. Geophys. Res., 98,* 7149-7163.

Donahue, N. M., Dubey, M. K., Mohrschladt, R., Demerjian, K. L., and Anderson, J. G. (1997) High-pressure flow study of the reactions OH+$NO_x \rightarrow HONO_x$: Errors in the falloff region. *J. Geophys. Res.* **102**, 6159-6168.

Gao, D., Stockwell, W. R., and Milford, J. B, (1995) First-order sensitivity analysis for a regional-scale gas-phase chemical mechanism. *J. Geophys. Res. 100*, 23153-23166.

Gao, D., Stockwell, W. R., and Milford, J. B, (1996) Global uncertainty analysis of a regional-scale gas-phase chemical mechanism. *J. Geophys. Res. 101*, 9107-9119.

Imre, D.G.; Daum, P.H.; Kleinman, L.; Lee, Y-N.; Lee, J. H.; Nunnermacker, L.J.; Springston, S.R.; Newman, L.; Weinstein-Lloyd, J.; and Sillman, S. Characterization of the Nashville urban plume on July 3 and July 18, 1995. Part II. Processes, efficiencies, and VOC and NO_x limitation. *J. Geophys. Res., in press.*

Jacob, D., NARSTO Critical Review: Heterogeneous chemistry and tropospheric ozone, *Atmos. Environ*, 1999 (in press)

Jeffries, H. E. and G. S. Tonnesen (1994) A comparison of two photochemical reaction mechanisms using mass balance and process analysis, *Atmos. Environ., 28*, 2991–3003.

Jeffries, H.E.; Sexton, K.G.; Arnold, J.R.; Bai, Y.; Li, J.L.; and Crouse, R. (1990) A chamber and modeling study to assess the photochemistry of formaldehyde. Report on EPA Cooperative Agreement CR-813964, Atmospheric Research and Exposure Assessment Laboratory, EPA, Research Triangle Park, NC.

Johnson, G. M. (1984) A simple model for predicting the ozone concentration of ambient air, *Proceedings of the 8th International Clean Air Conference*, Melbourne, Australia, pp. 715–731.

Kelly, N. A. (1985) Ozone/precursor relationship in the Detroit metropolitan area derived from captive-air irradiations and an empirical photochemical model, JAPCA, 35, 27-34.

Kleffmann, J., K. H. Becker, and P. Wiesen (1998) Heterogeneous NO_2 conversion processes on acid surfaces: Possible atmospheric implications, *Atmos. Environment, 32*, 2721-2729.

Kleinman L. I., P. Daum, J. H. Lee, Y.-N. Lee, L. Nunnermacker, S. Springston, J. Weinstein-Lloyd, L. Newman, and S. Sillman (1997) Dependence of ozone production on NO and hydrocarbons in the troposphere, *Geophys. Res. Lett., 24*, 2299-3202.

Milford, J., D. Gao, S. Sillman, P. Blossey, and A. G. Russell (1994) Total reactive nitrogen (NO_y) as an indicator for the sensitivity of ozone to NO_x and hydrocarbons, *J. Geophys. Res., 99*, 3533-3542.

Sillman, S. (1995) The use of NO_Y, H_2O_2, and HNO_3 as indicators for ozone-NO_x-hydrocarbon sensitivity in urban locations, *J. Geophys. Res., 100,* 14175-14188,.

Sillman, S. (1998) NARSTO Critical Review: The method of photochemical indicators as a basis for analyzing O_3-NO_x-ROG sensitivity. Submitted to *Atmos. Environ.*

Sillman, S.; Dongyang H.; Pippin, M.R.; Daum, P.H.; Lee, J.H.; Kleinman, L.I.; and Weinstein-Lloyd, J. (1997a) Model correlations for ozone, reactive nitrogen and peroxides for Nashville in comparison with measurements: Implications for O_3-NO_x-hydrocarbon chemistry. Submitted to *J. Geophys. Re*s.

Sillman, S.; He, D.; Cardelino, C.; and Imhoff, R.E. (1997b) The use of photochemical indicators to evaluate ozone-NO_x-hydrocarbon sensitivity: Case studies from Atlanta, New York and Los Angeles*, J. Air Waste Management Assoc. 47*:1030:1040.

Sillman, S., D. He, M. R. Pippin, P. H. Daum, D. G. Imre, L. I. Kleinman, J. H. Lee, and J. Weinstein-Lloyd (1998) Model correlations for ozone, reactive nitrogen and peroxides for Nashville in comparison with measurements: Implications for O_3-NO_x-hydrocarbon chemistry*, J. Geophys. Res. 103, 22,*629-22,644.

Simonaitis, R., and Bailey, E.M. (1995) Smog chamber studies at low VOC and NO_x concentrations: Phase I. Report on Interagency Agreement DW64936024 to EPA/NREL, Research Triangle Park, NC.

Stevens, P.S.; Mather, J.H.; Brune, W.H.; Eisele, F.; Tanner, D.; Jefferson, A.; Cantrell, C.; Shetter, R.; Sewall, S.; Fried, A.; Henry, B.; Williams, E.; Bagman, K.; Goldan, P.; and Kuster, W. (1997) HO2/OH and RO2/HO2 ratios during the Tropospheric OH Photochemistry Experiment: Measurement and theory*. J. Geophys. Res. 102***:**6379-6391.

Tonnesen, G. S. and R. L. Dennis, Analysis of radical propagation efficiency to assess ozone sensitivity to hydrocarbons and NO_x. Part 1: Local indicators of instantaneous odd oxygen production sensitivity, *J. Geophys. Res.*, in press.

Tonnesen, G. S., and R. L. Dennis, Analysis of radical propagation efficiency to assess ozone sensitivity to hydrocarbons and NO_x. Part 2: Long-lived species as indicators of ozone concentration sensitivity*, J. Geophys. Res.*, in press.